Polyacrylamide-treated kaolin: A fabric study

Sungho Kim, Angelica M. Palomino *

Department of Civil and Environmental Engineering, 226A Sackett Building, Penn State University, University Park, PA 16802, USA

ARTICLE INFO

ABSTRACT

Particle interactions, and in turn fabric, determine the behavior of clay mineral particle systems. Polymers with deliberately chosen characteristics, such as molecular mass and ionic type, can be utilized to manipulate clay fabric. The purpose of this study is to understand fabric development in a clay–polymer system, specifically kaolin–polyacrylamide systems over a wide range of solids content. Methodologies include sedimentation tests (low solids content), viscosity measurements (moderate solids content), and liquid limit measurements (high solids content), and are conducted to determine variation in fabric for kaolin–polyacrylamide systems at various concentrations, molecular mass and ionic types of polyacrylamide. Fabric development is verified using scanning electron microscopy (SEM). Results show that the polymer charge type impacts the resulting fabric formation only at polymer concentrations above a threshold concentration. Floc/aggregate size and density tend to increase with increasing polyacrylamide concentration, while high molecular-mass polyacrylamides tend to induce the formation of open flocculated structure. The most likely particle association in the presence of nonionic polyacrylamides is face-to-face association due to polymer bridging. A relationship is found between polymer characteristics, solids contents, and micro-scale particle arrangement. This study is relevant to the emerging field of engineered soil fabrics.

© 2009 Elsevier B.V. All rights reserved.

1. Introduction

Clay is one of the most important and commonly used natural materials for a wide range of applications including geo-environmental engineering and material science. Particle interactions, and in turn fabric, determine the behavior of clay systems. Clay fabric formation varies with the surrounding pore fluid environment, e.g., pH and ionic concentration (Rand and Melton, 1977; van Olphen, 1977; Theng, 1979; Pierre et al., 1995; Mitchell and Soga, 2005; Lagaly, 2006). Variation in pore fluid chemistry significantly influences interparticle forces and in turn particle associations. Clay fabric manipulation at the particle level can thus be accomplished by manipulating the pore fluid conditions, and thus the macro-scale clay properties that depend on fabric may be altered.

One method of pore fluid alteration is the use of polymer additives. Polymer adsorption on a clay mineral particle surface alters the surface properties of the particle, and hence forces between the particles (Theng, 1979). Polymers with deliberately chosen characteristics, such as molecular mass and ionic type, can manipulate clay fabric.

Polyacrylamide (PAM) is one of the most commonly used polymers in industrial applications. It is an inexpensive, highly effective agent for forming clay mineral particle–polymer flocs. PAM can be synthesized into various molecular masses and ionic forms. The difference in molecular mass and ionic type of PAM induces various bonding mechanisms between PAM molecules and kaolinite particles. A nonionic PAM molecule interacts with the surface of kaolinite particles via polymer bridging (Fleer et al., 1972; Theng, 1979; Chaplain et al., 1995; Carasso et al., 1997; Lagaly, 2006). The number of bonds between a clay mineral particle and a polymer molecule increases with increasing molecular mass. A cationic PAM molecule binds to negatively charged mineral surfaces and promotes particle aggregation through van der Waals attraction. This phenomenon is maximized at the critical coagulation concentration of the system, i.e. the minimum concentration of polymer that induces flocculation or aggregation (van Olphen, 1977; Theng, 1979).

An engineered kaolin system may be achievable with the addition of carefully chosen PAM molecules. The advantages of using PAM molecules are that they can be manufactured in a variety of charge types and chain lengths, and they adsorb irreversibly onto the clay mineral particle surface. The purpose of this fundamental study is to understand fabric development in kaolin–polyacrylamide systems by investigating the impact of charge type and chain length of polyacrylamide on the behavior of kaolin over a wide range of solids contents and strain conditions. Sedimentation tests (low solids content, zero strain condition), viscosity measurements (intermediate solids content, high strain condition), and liquid limit measurements (high solids content and high strain condition) are conducted to determine variation in fabric for kaolin–polyacrylamide system at various concentrations, molecular masses and ionic types of PAM. The resulting fabric at various solids contents are verified using scanning electron microscopy (SEM).

* Corresponding author. Tel.: +1 814 865 9427; fax: +1 814 865 8056.
E-mail address: amp26@psu.edu (A.M. Palomino).

2. Materials

2.1. Kaolin

The kaolin used in this study was an untreated kaolin from Wilkinson Kaolin Associates LLC (Gordon, Georgia). The chemical composition (Table 1) is approximately that of pure kaolinite as defined by Murray (1991) with a small content of impurities. The kaolin was converted to a monoionic sodium kaolin using a conversion method modified after van Olphen (1977). The method consists of mixing the kaolin in a 2 M NaCl solution for 48 h and a 1 M NaCl solution twice for 24 h each time. After the final salt wash, the excess salt was removed by replacing the supernatant fluid with deionized water until the supernatant conductivity measured less than 100 μS/cm. The converted kaolin slurry was oven-dried and ground using a pestle and mortar. Grain size distribution curves measured after the conversion are shown in Fig. 1. Selected properties of the kaolin are given in Table 2. The measured kaolin cation exchange capacity (CEC) was 2.3 cmol/kg (typical values for kaolin range from 1 to 10 cmol/kg — van Olphen, 1977). Impurities such as illite and smectite can increase the CEC, thus affecting polymer adsorption (Ma and Eggleton, 1999; Backfolk et al., 2006). The small content of impurity was confirmed to be illite as shown in the X-ray diffractogram (Fig. 2).

2.2. Polyacrylamide (PAM)

Clay mineral particle interactions were modified using three types of polyacrylamides: nonionic, low molecular mass nonionic, and cationic containing 20% cationic quaternary ammonium salt groups (Cytec Industries Inc., West Paterson, NJ). These polymer types were chosen to highlight the impacts of molecular mass and ionic type difference. Selected characteristics of the polymers are given in Table 3.

The influence of charge type was explored with a nonionic polyacrylamide (N-PAM) and a cationic polyacrylamide (C-PAM). The influence of polymer molecular mass was explored with a high molecular mass nonionic polyacrylamide (N-PAM) and a low molecular mass nonionic polyacrylamide (n-PAM). Polyacrylamides concentrations of 0, 20, 80, 120, 240, 500 mg/L were used to observe a change in behavior. The concentration range was selected based on calculated estimates of the influence of cationic PAM on the kaolinite particles surface charge and polymer charge (details can be found in Kim (2008)).

3. Experimental methods

3.1. Sedimentation tests

The relative state of dispersion and particle association types of low solids content slurry can be inferred from observing settling behavior
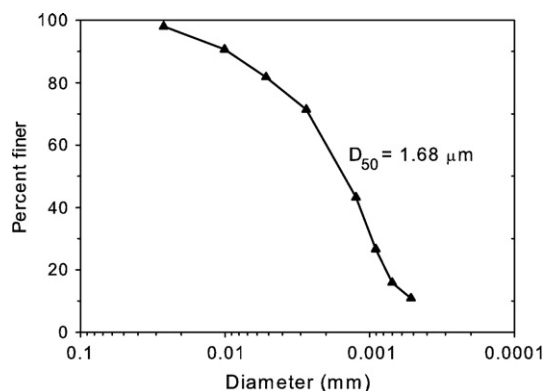

Fig. 1. Particle size distribution curve for monoionic kaolin used for this study. Data obtained using ASTM D422-63 (2003).

and relative final sediment volume. Observable settling modes are defined herein as (after Palomino and Santamarina (2005)):

- Edge-to-face (EF) flocculated settling: the dispersion has a uniform density, a clear supernatant, a well-defined supernatant-dispersion interface that moves downward, a rapid settling rate, and a voluminous final sediment.
- Face-to-face (FF) aggregated settling: the dispersion appears to have a uniform density, a clear supernatant, a well-defined supernatant–dispersion interface that moves in a downward direction, a very rapid settling rate, and a compact final sediment relative to EF flocculated settling.
- Dispersed settling: the particles have minimal interaction, the dispersion initially has a milky appearance that changes to increasing density with time, from top to bottom, a cloudy supernatant, a well-defined dispersion–sediment interface that very slowly moves upwards, and a compact final sediment.
- Mixed-mode sedimentation is defined when the settling behavior exhibits characteristics of both flocculated and dispersed settling.

The induction period is defined as the slope of the initial phase of the sediment height–time curve and can be used to infer particle association type. For example, a flocculated system settles rapidly and has a short induction time, and a dispersed system has a very long induction period. Eqs. (1) and (2) established from correlations between the settling rate of a dispersion–sediment interface and the volume of the final sediment provide an indication of floc density and size when flocculation or aggregation occurs as well as when the particles remain dispersed in the system. Particle associations can also be inferred through estimations of floc size and density calculated from the sedimentation test results. Floc density (ρ_f) and diameter

Table 1
Comparison between chemical compositions of kaolin used for this study and pure kaolinite.

Constituent	% constituent	
	Kaolin (manufacturer data)	Kaolinite (Murray, 1991)
SiO_2	45.6	46.3
Al_2O_3	38.4	39.8
Fe_2O_3	0.4	
TiO_2	1.5	
CaO	0.06	
MgO	Trace	
K_2O	0.18	
Na_2O	Trace	
LOI	13.82	13.9

Table 2
Properties of kaolin.

Property	Value
Median particle diameter, D_{50} (μm)	1.68
Specific gravity	2.6
Specific surface[a] (m^2/g)	40.37
pH (at solids content of 2%)	7.5
Isoelectric point (pH)[b]	2.3
Cationic exchange capacity (cmol/kg)[c]	2.3
Viscosity (7% solids at pH = 6, mPa·s)[d]	8.88

[a] Methylene blue European spot method (Santamarina et al., 2002).
[b] Determined from zeta potential measurements using a PALS zeta potential analyzer (Brookhaven Instruments Co.).
[c] Ammonia-electrode method (Borden and Giese, 2001).
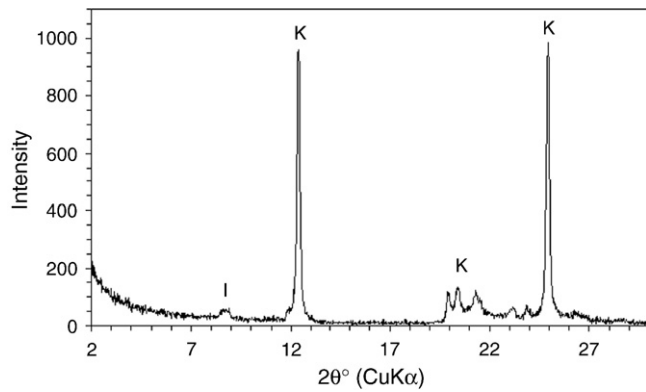[d] Brookfield #S00 spindle at 100 rpm.

Fig. 2. XRD patterns of the kaolin used in this study, obtained using Scintag2 PAD V, Scintag Inc., Cupertino, CA. I denote illite and K denotes a typical reflection for kaolinite.

(D) can be calculated as (Richardson and Zaki, 1954; Godard and Richardson, 1969; Bhatty et al., 1978; Font et al., 1999)

$$\rho_f = \frac{\rho_s + (k-1) \cdot \rho_L}{k} \tag{1}$$

$$D = \left(\frac{18\mu \cdot \mu_u}{g(\rho_f - \rho_L)} \right)^{0.5} \tag{2}$$

where ρ_s is the particle solid density, ρ_L is the dispersion fluid density, μ is the fluid viscosity (0.01 poise for water at 20 °C), k and μ_u are parameters obtained from the relationship between settling rate and solids content in terms of volume:

$$V_s^{1/n} = -k \cdot \mu_u^{1/n} + \mu_u^{1/n} \tag{3}$$

where V_s is settling rate ($-dh/dt$) and n is the flow regime parameter (4.65 for rigid particles). Because of the buoyancy effect (the resistance to settling increases with increasing floc volume), both floc size and density are considered in conjunction with the settling behavior (Kaya et al., 2006).

Sedimentation dispersions were prepared with a final solids content (ϕ) of 0.02 to minimize particle collisions that induce hindered settling (Irani and Callis, 1963). The solids content is defined as the proportion of solids volume with respect to the total dispersion volume. The initial pH and ionic concentration were held constant for all sedimentation tests at pH 6 and zero ionic concentration (deionized water) prior to polymer addition. PAMs with differing molecular mass and ionic type were added at various concentrations. Under constant pore fluid pH and low ionic concentration, particle interactions were governed by the polymer characteristics and dosage of the polymer.

The total volume of each test suspension was 100 ml. 5.2 g of kaolin were placed in a 200 ml beaker and mixed with deionized water. The beaker was placed on a Corning magnetic stirrer and was hydrated for 24 h before the pH adjustment. The dispersion pH value was modified by adding either 0.2 M hydrochloric acid (HCl) or 0.2 M sodium hydroxide (NaOH) until the dispersion pH reached the target pH 6 at which the kaolinite particles have no net charges at the edge, i.e., the point of zero edge charge (Dollimore and Horridge, 1973; Kretzschmar et al., 1998). The initial pH 6 and zero ionic concentration were held constant. The beaker was placed on the stirrer, and the suspension was mixed with various concentrations of PAMs for another 24 h prior to the sedimentation test. During the hydration process, the dispersion was covered to prevent evaporation. The dispersion was transferred to a 28 mm-inner diameter graduated glass cylinder. Entrapped air in the dispersion was removed with a low vacuum ($u \approx -0.01$ Pa, Duo Seal vacuum pump from Welch Scientific Company, IL) until no bubbles were seen. The vacuum was removed and the cylinder was capped with a rubber stopper. The solids were resuspended by repeatedly inverting the cylinder for 1 min.

The settling behavior, dispersion height, and sediment height were monitored with time. The heights were recorded for at least 3 weeks starting at $t = 1$ min: time intervals are 1, 2, 4, 8, 15, 30, 60 min, 2, 3, 6, 18 h, 1 day, 2 days, 4 days, 1 week, 2 weeks, and 3 weeks. The supernatant pH and conductivity of each dispersion were measured using an Accumet XL50 pH and conductivity meter (Fisher Scientific) after the last dispersion and sediment heights were recorded.

3.2. Viscosity measurement

In slurries, dispersed particles promote higher viscosities than that of the pure fluid phase because particles induce fluctuations in the stream lines even under laminar conditions. The concentration of the dispersed solids, the size and shape of the dispersed particles, and the interaction forces between the particles influence the rheological properties of dispersed systems (Hunter, 1993). In other words, viscosity measurements for particulate systems give an indication of

Table 3
Characteristics of polyacrylamides used in this study.

Type	Trade name	Structure (Huang et al., 2001)	Fraction of charged units	Molecular mass (g/mol)[a]
Nonionic	N300		None	~6×10^6
Nonionic (low molecular weight)	N300LMW		None	~8×10^4
Cationic	C494		$\frac{b}{(a+b)} \cong 0.2$	~4×10^6

[a] Measured using the viscometry method (Brandrup and Immergut, 1989; Ravve, 2000).

stability or flocculation of the dispersion. At moderate solids content, flocculated kaolinite particle dispersions have a much higher viscosity than that of well-dispersed kaolinite particle dispersions due to the greater energy required to overcome the shear deformation resistance. Rheological behavior of clay mineral particle dispersions is typically between shear-thinning and near-Newtonian behavior. Shear-thinning occurs when the number of interparticle bonds in a flocculated dispersion decreases with increasing shear rate. Thus, the shear-thinning rheological behavior of clay mineral particle dispersions can be regarded as mechanical deflocculation (Rand and Melton, 1977; Hunter, 2001). Near-Newtonian behavior indicates a system nearly free of flocs.

All the mixtures prepared for this rheological study had a solids content of 0.07. The temperature was monitored throughout and remained fairly constant at 21.5 °C ± 2 °C. For each test, the appropriate solids mass (91 g kaolin) for forming a dispersion with a solids content (ϕ) of 0.07 was placed in a 600 ml beaker. The total volume of the dispersion was 500 ml. The beaker was placed on a Corning magnetic stirrer and hydrated with deionized water for 24 h before pH adjustment. The suspension pH value was modified by adding either 0.2 M hydrochloric acid (HCl) or 0.2 M sodium hydroxide (NaOH) until the target pH 6 was reached. The beaker was placed on the stirrer mixing with various concentrations and ionic types of PAMs for another 24 h prior to measurement. The suspensions were covered to prevent evaporation.

Viscosity was measured using a Brookfield LVDV-1 Prime Viscometer fitted with spindles #00, 61, or 62, depending on the suspension viscosity and spindle measurement range. Spindle #00 had the largest diameter and was therefore used to measure fluids with very low viscosity (1–600 mPa·s). The spindle rotational speed was varied between 1 rpm and 100 rpm, and the viscosity reading was recorded at 30-second intervals for each rotational speed setting. Between readings, the dispersions were mixed for 20 s to counteract particle settlement. The final pore fluid pH was determined by centrifuging a small sample (10 ml) and measuring the supernatant.

3.3. Liquid limit measurement

The liquid limit can be used to infer fabric because the shear strength of clay at its liquid limit is dependent on the soil fabric (Wroth and Wood, 1978; Mitchell, 1993). The liquid limit is the water content of a soil at the boundary between the plastic and liquid behavioral states. Soils at the liquid limit have a shear strength ranging from 2.4 kN/m² to 1.3 kN/m² over the liquid limit range of 30%–200% (Wroth and Wood, 1978). A higher liquid limit implies that flocculated fabric dominates the system. An edge-to-face flocculated fabric resists shear more than a face-to-face aggregated or a dispersed fabric. Aggregated and dispersed fabrics tend to have relatively lower liquid limits (Mitchell, 1993). Manipulating pore-fluid chemistry by varying polymer type and concentration will alter the soil shear strength, and in turn the liquid limit. The sensitivity to pore fluid changes is indicated by the slope of the measured penetration depth–water content lines. As the slope increases, the soil shear strength reduces rapidly for a given increase in water content.

The liquid limit was determined with the fall cone test, BS1377-1 (BSI, 1990). The test was performed using a Humboldt penetrometer (model number: H-4236, Humboldt Mfg. Co., IL). According to the British Standard, liquid limit is defined as the water content at which 80 g stainless steel cone with a 30° angle penetrates a remolded soil specimen 20 mm from the soil surface.

3.4. Scanning electron microscopy study

SEM provides direct images of the particle systems, thus allowing for fabric development verification. A freeze-drying technique was adopted to preserve the soil fabric by bypassing the effects of capillary

forces. Sample surfaces were coated with a conductive material, gold, using a sputter-coater to increase the surface electrical conductivity and improve the image quality. Samples of kaolin-PAM composites were observed in an SEM S-3500 N (Hitachi Inc.).

4. Results

4.1. Settling behavior

Settling behavior for both supernatant–dispersion and dispersion–sediment boundaries are plotted in Fig. 3. Based on observed settling
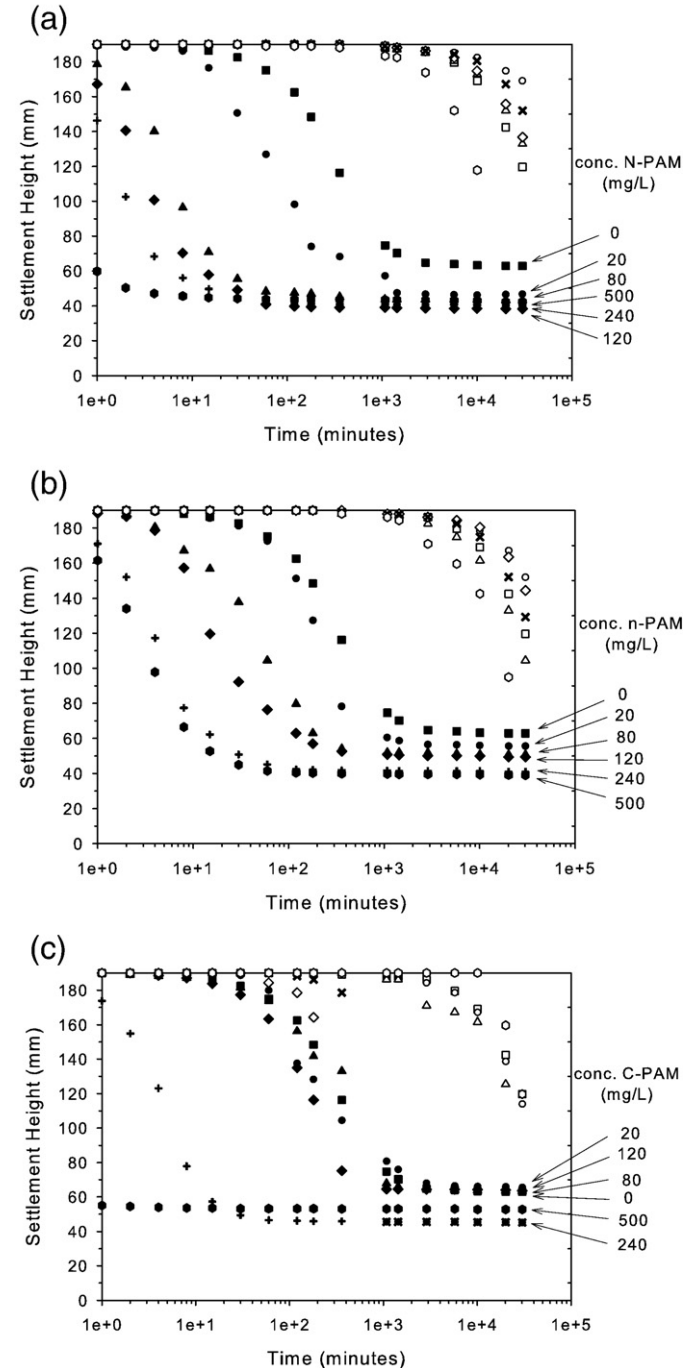

Fig. 3. Plot of sedimentation boundary height with time for pure kaolin and kaolin-PAM dispersions: (a) N-PAM, (b) n-PAM, and (c) C-PAM. Open symbols and x denote supernatant–dispersion boundaries while closed symbols denote dispersion-sediment boundaries. After a long time t, the two boundaries are expected to meet, except for the case of true dispersed behavior.
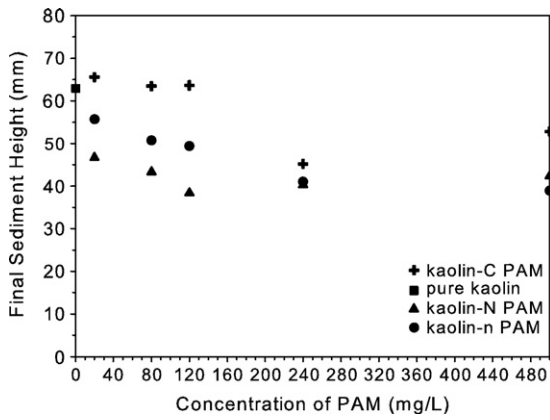
Fig. 4. Final sediment height measured at time = 3 weeks.

characteristics, all tested dispersions, except 120 mg/L C-PAM, were characterized as mixed-mode and tended to become FF aggregated with increasing PAM concentration. At C-PAM concentration of 120 mg/L, the dispersion settling-characteristics were consistent with FF aggregation sedimentation. The molecular mass of PAM influenced the settling behavior of dispersion–sediment boundary. The dispersion–sediment boundary settled more rapidly in the presence of high molecular PAM (N-PAM and C-PAM).

The final sediment heights for each dispersion are compared in Fig. 4. At PAM concentrations less than 120 mg/L, the final sediment height decreased with increasing PAM concentration. The n-PAM (low molecular mass) resulted in a more open sediment than N-PAM (high molecular mass) at lower concentrations, while little change was observed for n-PAM and N-PAM at higher concentrations. C-PAM induced a more voluminous sediment at 500 mg/L. In the presence of C-PAM, nearly the same final sediment heights were observed at concentration less than C-PAM 120 mg/L, above which the height significantly decreased. At C-PAM concentrations above 240 mg/L, the final sediment height again increased implying the formation of higher order EF flocs through FF aggregate linkages. The molecular mass influenced final sediment height at low PAM concentrations ranging from 20 to 120 mg/L, i.e. the final sediment height decreased with increasing molecular mass. In the experimental range of PAM concentration, nonionic PAM (both N-PAM and n-PAM) formed denser structures than cationic PAM. For all three polymers tested, the final sediment heights had similar values at PAM concentration of 240 mg/L. Furthermore, the fabric densified in the C-PAM and n-PAM cases, indicating a higher ratio of FF aggregates.

Floc diameters and densities calculated using Eqs. (1) and (2) are summarized in Table 4. With increasing nonionic PAMs concentration, floc diameter and density increased until the sediment height reached a minimum, i.e. FF aggregation-dominated. In the presence of C-PAM, the floc diameter tended to increase with increasing PAM concentration. The lowest final sediment height and maximum calculated floc density occurred at PAM concentration of 240 mg/L.
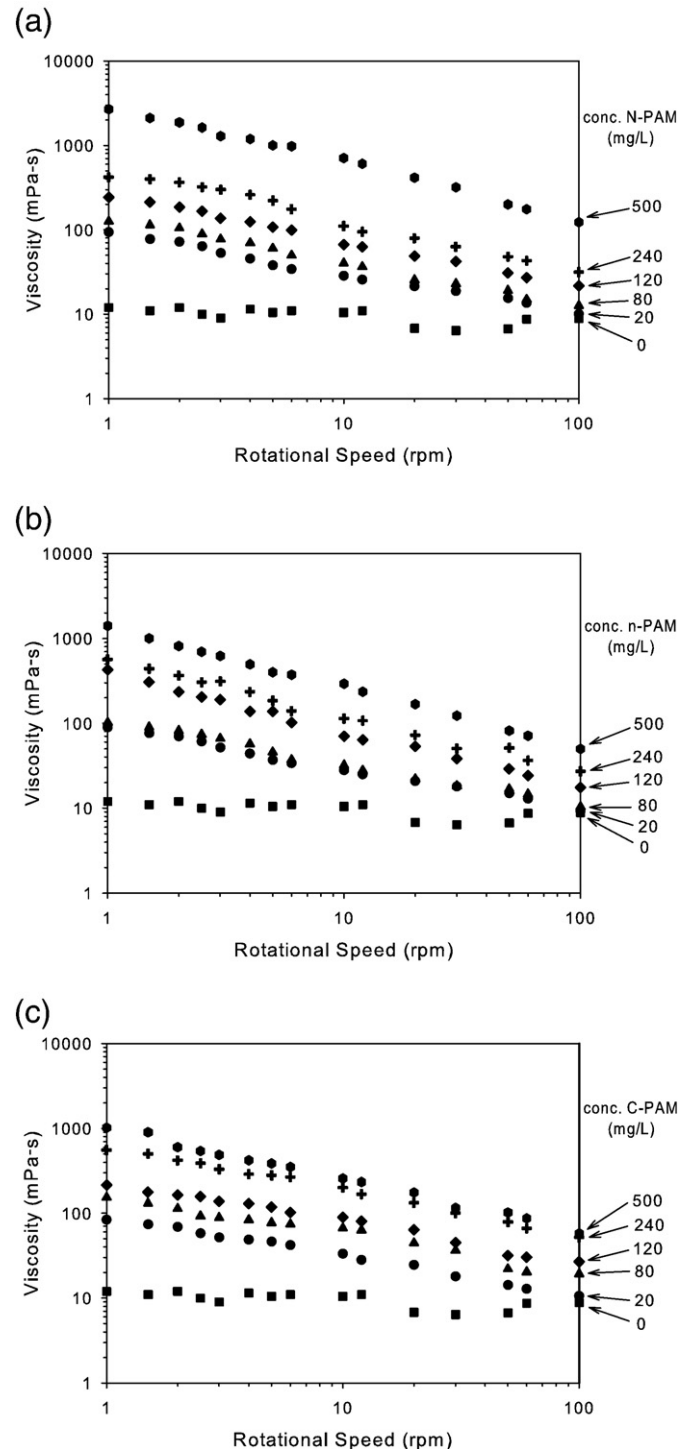
(a)

(b)

(c)

Fig. 5. Viscosity measurement for pure kaolin and kaolin-PAM suspensions at rotational speeds of 1–100 rpm: (a) N-PAM, (b) n-PAM, and (c) C-PAM. Measurements taken with spindle S61 and S62.

Table 4
Floc size and density calculated from sedimentation tests.

Polymer type	PAM concentration (mg/L)	Induction rate (mm/min)	Floc density (g/cm³)	Floc diameter (μm)	Final sediment height (mm)
Pure kaolin	0	0.24	1.118	4.0	62.89
N-PAM	20	0.48	1.153	7.1	46.74
	80	11.4	1.154	26.6	43.32
	120	22.8	1.178	29.0	38.38
	240	43.7	1.164	52.2	40.28
	500	130.2	1.143	634.7	42.37
n-PAM	20	0.29	1.138	4.6	55.67
	80	1.5	1.142	10.5	50.73
	120	1.7	1.139	16.8	49.40
	240	19	1.166	28.8	41.04
	500	28.5	1.173	32.8	38.95
C-PAM	20	0.04	1.110	7.1	65.55
	80	0.31	1.137	3.4	63.46
	120	0.41	1.125	6.3	63.65
	240	16.1	1.155	34.2	45.22
	500	134.9	1.115	9621	52.82

4.2. Viscosity

All PAM-treated dispersions exhibited a typical shear-thinning behavior as shown in Fig. 5. The viscosity profiles were interpreted as follows: the greater the dispersion viscosity, the more flocculated the suspension is relative to the other test cases.

The viscosities at the maximum tested shear rate, 100 rpm, are shown in Fig. 6. Viscosity data at 100 rpm were used as the comparison viscosity at maximum shear rate. Viscosity increased with increasing PAM concentration. In the presence of C-PAM, the suspensions increased in viscosity with increasing C-PAM concentration until reaching a nearly constant value at 240 mg/L. At PAM concentration above 240 mg/L, N-PAM-treated suspension had the greatest viscosity. The ionic group of C-PAM had a greater effect on viscosity than the molecular mass did at PAM concentration from 20 to 240 mg/L. However, the molecular mass of PAM became a significant factor at PAM concentration above 240 mg/L.

4.3. Liquid limit

Cone penetration lines for each sample measured using the fall cone test are shown in Fig. 7. n-PAM had very little influence on penetration depth–water content relationship. The liquid limits and liquid limit line slopes are plotted in Fig. 8. Liquid limit increased with an increase in PAM concentration. Only slight differences between C-PAM and N-PAM were observed, while n-PAM-treated specimens had a lower liquid limit trend across the tested concentrations. A higher slope corresponded to a high molecular mass PAM, i.e. N-PAM and C-PAM, at intermediate PAM concentration. At 20 and 500 mg/L of all PAM types, the liquid limit trend lines had nearly the same slope indicating fairly insensitive behavior to water content in the presence of the polymers.

5. Discussion

5.1. Influence of polymer molecular weight

Polymer bridging is the dominant bonding mechanism between a nonionic polymer molecule and a kaolinite particle (Theng, 1979; Pefferkorn et al., 1985; Gregory, 1988; Mpofu et al., 2003). A nonionic PAM molecule can be adsorbed onto both face and edge sites of kaolinite particles. However, the most likely particle association is FF in the presence of nonionic PAM due to a much larger proportion of face area compared to edge area on the kaolinite particle. The estimated ratio of edge area to the whole particle surface area is 0.127 based on the SEM images. Bridging between particles occur when polymer molecules link two or more particles together. Thus, it is
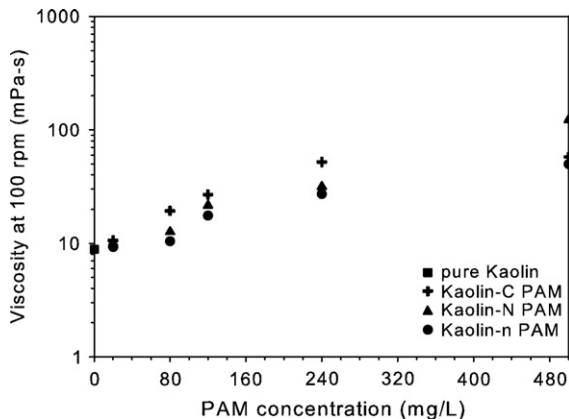

Fig. 6. Viscosity data for all dispersions at 100 rpm using Spindle S61 and S62.
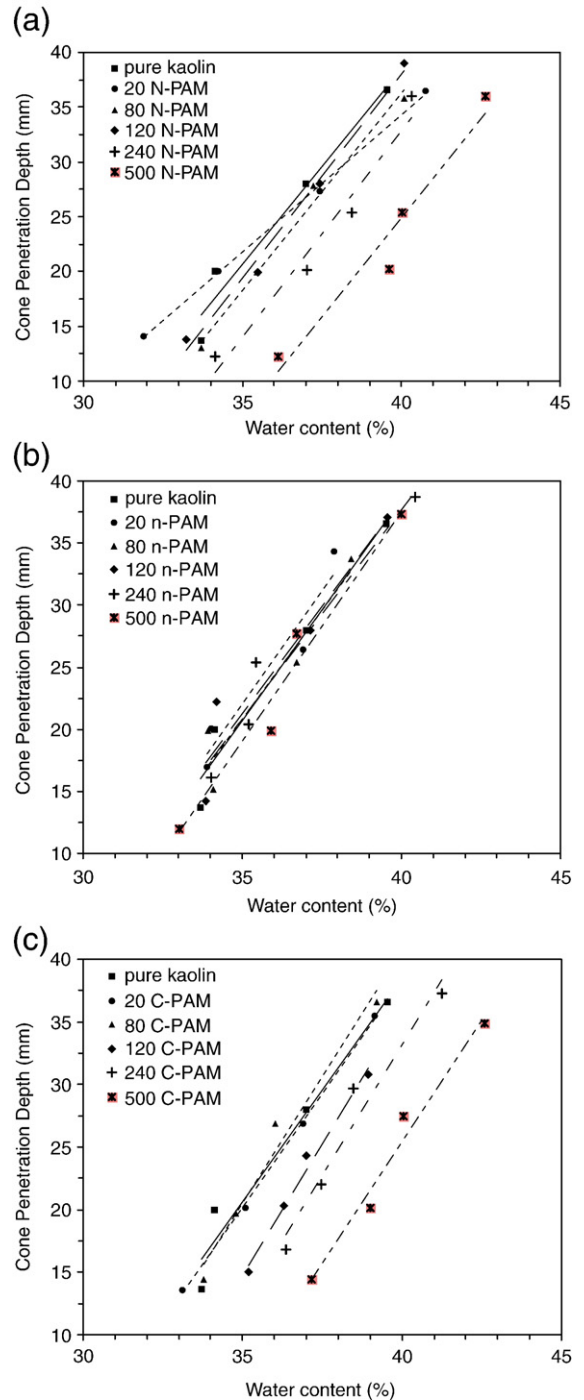

Fig. 7. Liquid limit lines for PAM-treated kaolin specimens at various PAM concentrations: (a) N-PAM, (b) n-PAM, and (c) C-PAM.

more likely that the polymer molecules bind to the face of at least one particle and bridge with another particle via face adsorption.

The number of FF aggregates increased with increasing PAM concentration and molecular mass in the tested low solids content dispersions, as shown in Fig. 9. All nonionic PAM-treated dispersions had mixed-mode sedimentation behavior which includes both dispersed characteristics and flocculated/aggregated characteristics. The ratio of flocculated/aggregated particles to dispersed particles, for a given polymer type, increased with increasing PAM concentration.

The final sediment height (Fig. 4) and induction rate (Table 4) also indicated an increase in FF aggregation with increasing PAM concentration. The induction rate increased with increasing PAM

(a)

Liquid Limit (%)

- pure Kaolin
- Kaolin-N PAM
- Kaolin-C PAM
- Kaolin-n PAM

PAM concentration (mg/L)

(b)

Slope of Liquid Limit Line

- pure Kaolin
- Kaolin-C PAM
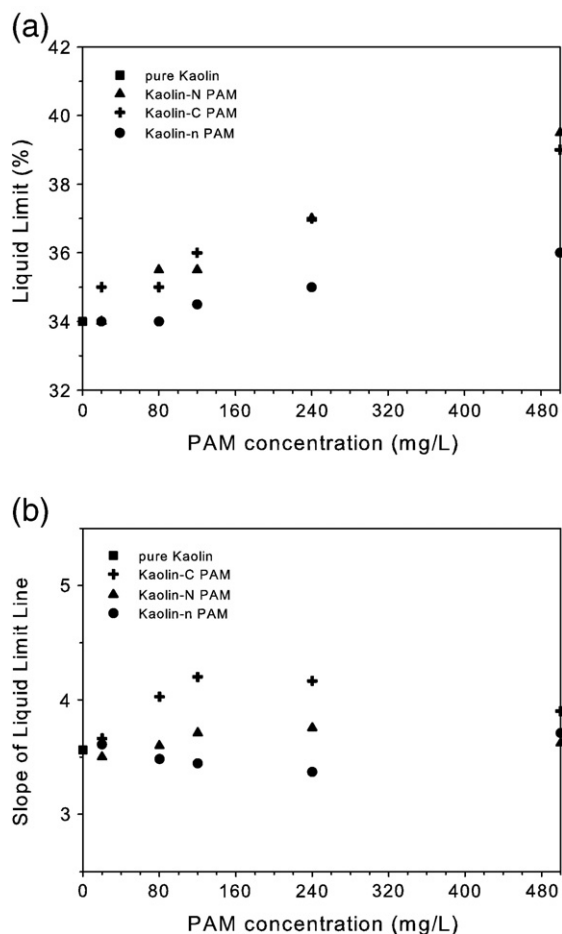- Kaolin-N PAM
- Kaolin-n PAM

PAM concentration (mg/L)

Fig. 8. (a) Liquid limit for all mixtures of kaolin with various concentrations of PAMs. (b) Slopes of the fall cone liquid limit lines.

concentration, indicating flocculated/aggregated fabric formation. The final sediment height decreased with increasing PAM concentration up to 120 mg/L for high molecular mass nonionic PAM, and 240 mg/L for low molecular mass nonionic PAM. Hence, these concentrations are apparent optimum concentrations for the densest sediment at solids content of 0.02, indicating the highest ratio of FF aggregates.

By definition, the higher molecular mass nonionic PAM had more monomer units per molecule (longer chain length) than the low molecular mass nonionic PAM. When comparing the final sediment height, the ratio of FF/EE associations (dense structure) to EF associations (open structure) was higher for high molecular mass nonionic PAM than that for low molecular mass nonionic PAM. In addition, higher molecular mass nonionic PAM formed larger denser flocs according to the floc size and density calculations. This is verified in Fig. 10 where larger flocs, at the same magnification, were observed in the presence of high molecular mass nonionic PAM than low molecular mass nonionic PAM. Hence, a higher molecular mass led to a more aggregated and compact sediment compared to the low molecular mass polymer case.

At intermediate solids content, the molecular mass of PAM also greatly impacted viscosity. The pure kaolin case had dispersed characteristics while, nonionic PAM-treated dispersions showed shear thinning behavior. Viscosity, and therefore flocculation/aggregation increased with increasing PAM concentrations (n-, N-, and C-PAM) and with molecular mass. Higher viscosity resulted from larger flocs formed in the presence of a higher molecular mass nonionic PAM.

For high solids content, the high molecular mass PAM had a greater influence than low molecular mass PAM. The liquid limit significantly increased with increasing high molecular mass PAM concentration, while the liquid limits were nearly the same in the presence of low molecular mass PAM. Particles were linked together with polymer molecules, leading to flocs and aggregates. In a flocculated system, water becomes trapped within and between open flocs. A more flocculated, voluminous fabric can accommodate more water, thereby increasing the liquid limit (Mitchell, 1956). With increasing polymer concentration, a more open fabric was observed at the micro-scale (Fig. 11). In addition to water trapped within the particle flocs and pores, PAM molecules are hydrophilic and so provided additional adsorption sites for water molecules. This phenomenon resulted in a higher liquid limit and was more likely at a higher polymer concentration for all tested types of PAM. The slope of fall cone liquid limit lines (an indicator of sensitivity to water content) did not vary significantly with PAM concentration for all tested types of PAM. The presence of PAM molecules helped prevent shear strength from abruptly decreasing when water content increased.

5.2. Influence of polymer ionic type

Coulombian attraction is the dominant bonding mechanism between the clay surface and cationic PAM molecules (van Olphen, 1977; Theng, 1979; Laird, 1997). The positively charged trimethyl ammonium groups of cationic PAM are attracted to the negatively charged sites along clay mineral particle surface. At the critical coagulation concentration (CCC) of the PAM-treated kaolin systems, all charges on the mineral surface were compensated. Once the CCC was reached, aggregation occurred through van der Waals attraction. The charged groups of cationic PAM may have also adsorbed onto more than one particle, and so contributed to polymer bridging.

At cationic PAM concentration of 120 mg/L, clear FF aggregated settling behavior was observed indicating that 120 mg/L was at or near the CCC. At PAM concentration above 240 mg/L, the final sediment height of cationic PAM increased with increase in PAM concentration while that of nonionic PAM remained nearly constant. This may be explained according to the charge reversal effect (Lagaly, 2006) demonstrated by the calculation of charge density and number of available charges on the PAM molecules (calculation details can be found in Kim (2008)). 5.2 g of kaolin used for a dispersion with solids content of 0.02, which has approximately 2×10^{19} available sites, interacts with the same number of cationic groups of cationic PAM at a concentration of 164 mg/L to balance all the available particle surface charge. Charge neutralization should have occurred between the tested 120 and 240 mg/L of cationic PAM concentration. Therefore, charge reversal may have occurred at PAM concentration of 240 mg/L, and repulsive forces between PAM-adsorbed particles increased with increasing cationic PAM concentration at PAM concentration above 240 mg/L. Although the CCC of PAM-adsorbed kaolin should be equivalent to the CEC value (Penner and Lagaly, 2000), the measured CEC value showed much higher capacity for charge compensation (1.2 mmol/L) than the equivalency for the number of cationic groups of PAM at the calculated CCC (8.2×10^{-6} mmol/L). This may result from significant reduction of surface potential by the organic cation adsorption (Penner and Lagaly, 2000). This decrease in surface potential decreased the repulsive forces between PAM-adsorbed particles, thus promoted the particles to link before the CEC-based equivalency was reached.

Once charge neutralization was reached, long-range van der Waals forces and short-range ion–dipole interactions dominated the system. This resulted in FF aggregate formation. At concentrations above the CCC, hydrogen bonding between the molecule and mineral surface, which mainly occurs at edge sites, became the dominant bonding mechanism due to the lack of available exchangeable cations at the face sites. Aggregates linked together with excess cationic PAM molecules through polymer bridging and hydrogen bonds forming
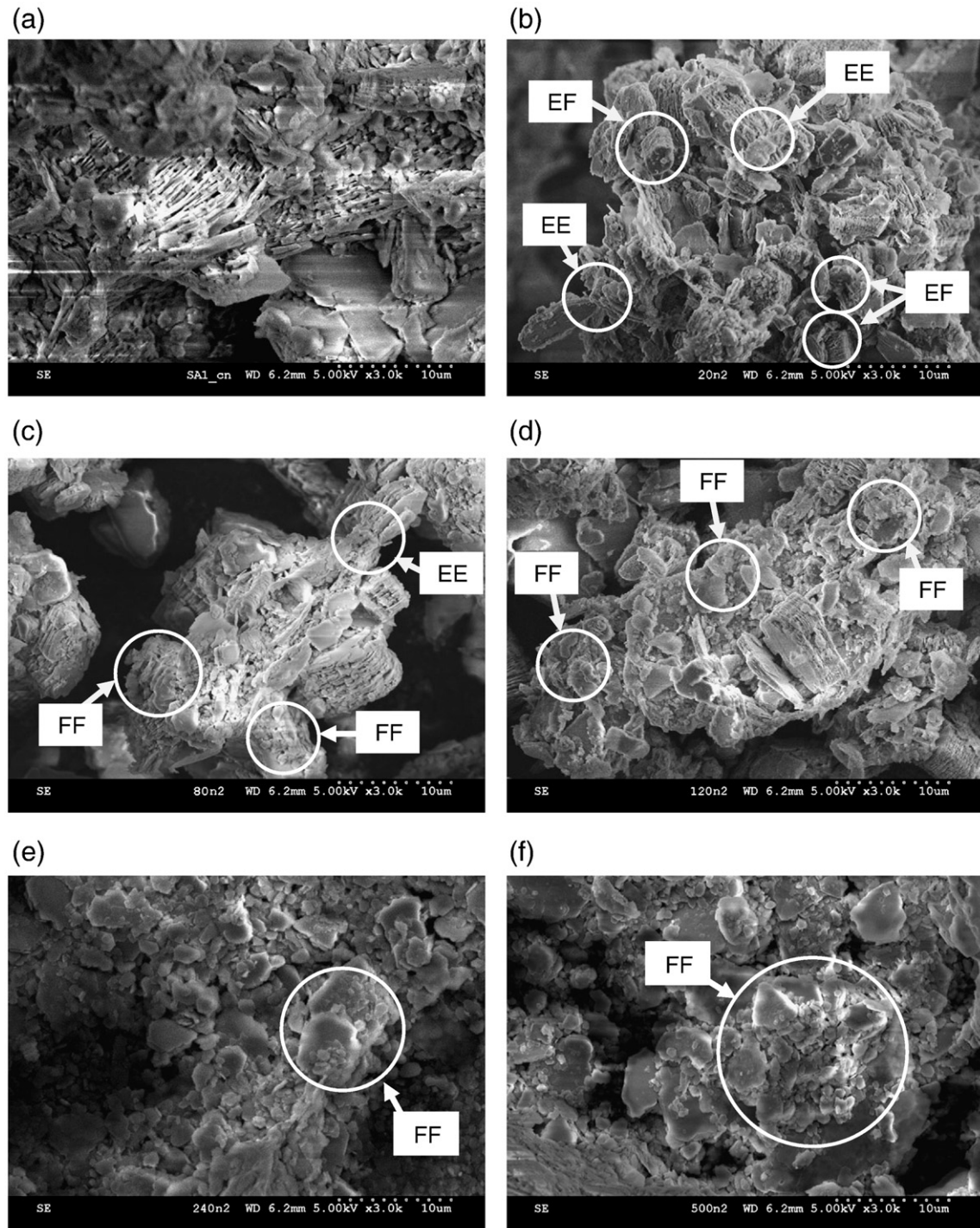
Fig. 9. SEM images, at $\phi = 0.02$, in the presence of n-PAM varying with concentrations: (a) 0 mg/L, (b) 20 mg/L, (c) 80 mg/L, (d) 120 mg/L, (e) 240 mg/L, and (f) 500 mg/L.

higher-order EF or EE structures. Such association development is likely because the kaolin particle surface charge is compensated and hydrogen bonds can dominate instead of stronger ion–dipole interactions (Israelachvili, 1991; Ebnesajjad, 2006). These higher-order EF flocs had a greater volume than EF flocs formed by single particles. The stacking of these higher-order structures led to an increase in final sediment height. A more open structure (EF and EE) formed in the presence of cationic PAM is seen in Fig. 12. FF aggregation formation was also interpreted through the floc size and density analysis (Table 4). The floc density of cationic PAM-treated dispersions abruptly increased at PAM concentration above 120 mg/L. This

phenomenon corresponded to the lowest sediment height at PAM concentration of 240 mg/L.

Although the CCC for solids content of 0.07 is theoretically 574 mg/L (not tested in this study), cationic PAM-treated kaolin dispersions had a higher viscosity than nonionic cases at PAM concentration below the CCC. This may have been due to a higher bonding energy of ion-related bonds, such as Coulombian attraction and ion–dipole interaction, than that of non-ion-related bonds such as hydrogen bonds and hydrophobic bonds. A greater molecular interaction force resulted in an increase in flocculation, and thus a higher viscosity. The observation that the higher CCC was shown at the higher solids
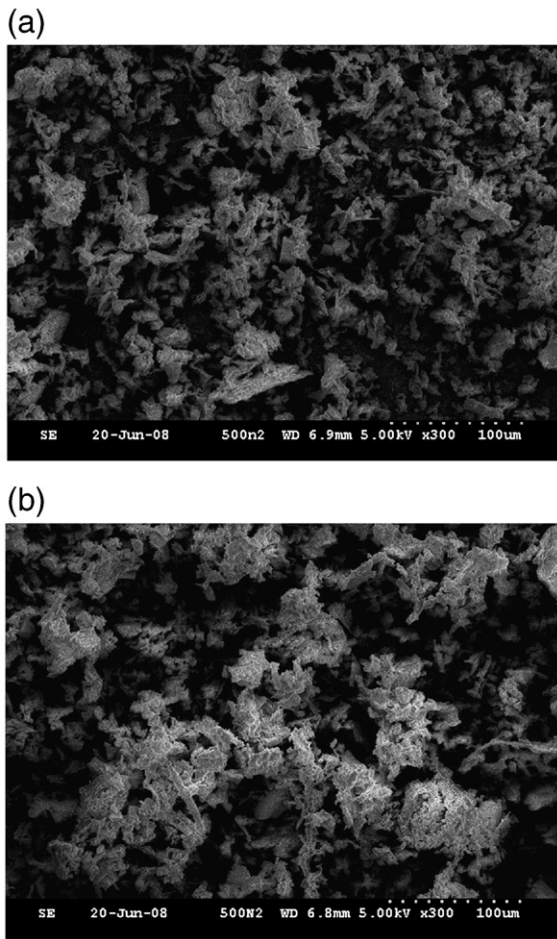
(a)

(b)

Fig. 10. SEM images in the presence of (a) 500 mg/L n-PAM and (b) 500 mg/L N-PAM, at $\phi = 0.02$.

(a)

(b)

Fig. 12. SEM images in the presence of 500 mg/L of (a) N-PAM and (b) C-PAM, at $\phi = 0.02$.

content, 0.07 is consistent with previous studies that CCC increases with increasing solid content (Williams and Drover, 1967; Penner and Lagaly, 2000; Lagaly, 2006).

While the molecular mass of PAM influenced the tested high solids content systems, the effect of ionic type was insignificant in the tested range of PAM concentrations. Due to the relatively very low number of charges of the cationic PAM compared to that of the total surface area of the kaolinite particles at high solids content, the impact of positively charged groups of PAM became less important at high solids
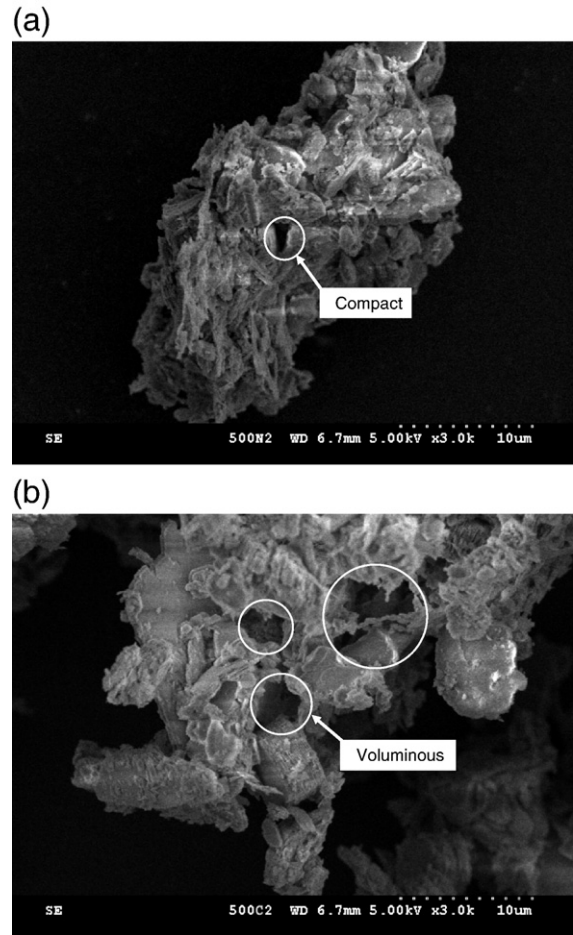
content (>0.4). This was evidenced by only a slight difference in liquid limit between N-PAM-treated kaolin mixtures and C-PAM-treated kaolin mixtures. This indicated that polymer bridging was a more effective bonding mechanism than electrostatic forces at very high solids content.

6. Conclusions

Particle interactions, and in turn fabric, determine the behavior of clay mineral particle systems. Polymers with deliberately chosen
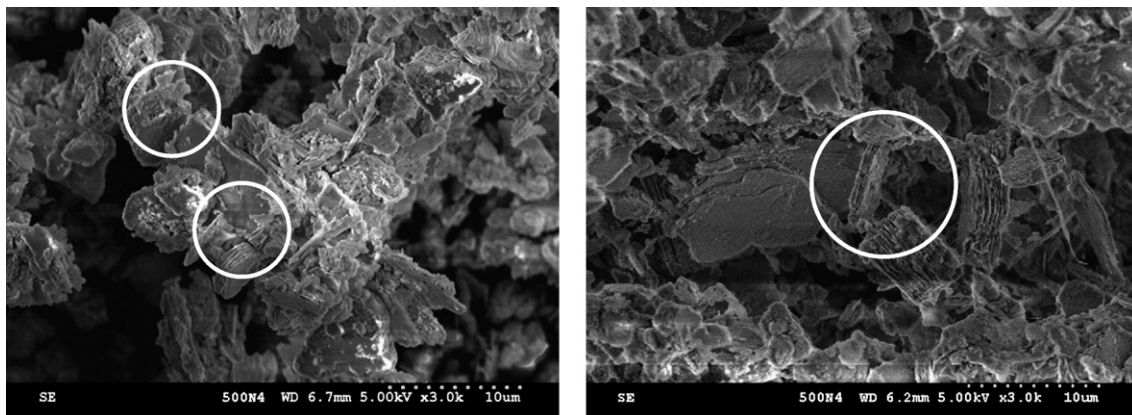

Fig. 11. EF and open EE associations in the presence of 500 mg/L N-PAM, at $\phi > 0.4$.

characteristics, such as molecular mass and ionic type, can manipulate clay fabric. Once polyacrylamide molecules bind to kaolinite particles, the adsorption strongly alters the clay mineral particle surface characteristics, leading to altered particle associations and therefore altered fabric. Macro-scale tests, representing a wide range of solids contents, were used to infer fabric resulting from various particle associations. Clay fabrics were verified with scanning electron microscopy.

The molecular mass of polyacrylamide had a greater impact on kaolin fabric formation than charge type. A higher molecular mass and polymer concentration resulted in a greater number of monomer units per single polymer chain, compared to a lower molecular mass and polymer concentration. With increasing number of monomer units in the system, more polymer bridges can form leading to a more flocculated system. This was evidenced by an increase in face-to-face (FF) aggregation with increasing nonionic polymer molecular mass (high molecular mass versus low molecular mass) and concentration at the same solids content. FF aggregation was the dominant particle association in the nonionic polyacrylamide-treated kaolin systems. More polymer bridges induced a greater proportion of FF aggregates which manifested as a denser final sediment.

Although to a lesser degree, the ionic type of polyacrylamide also influenced kaolin fabric formation. At cationic polymer concentrations above the critical coagulation concentration (CCC), FF aggregates formed higher-order edge-to-face (EF) floc structures by linking FF aggregates. The CCC was determined by the ratio between number of available mineral surface charges and number of charged polymer monomer units. At the CCC, the cationic polyacrylamide-treated kaolin system had the densest final sediment height due to FF aggregation. The final sediment height increased at polymer concentrations above the CCC, corresponding to larger flocs and a more open fabric. This finding was consistent with the floc size and density analysis performed in this study. At low cationic polymer concentrations, significant differences in macro-scale behavior were observed, while at high solids content nearly the same macro-scale behavior was observed as in the pure kaolinite case.

Polyacrylamide contributed to higher liquid limits, compared to the pure kaolin case. The polymer molecules bound formed FF aggregates leading to higher-order of EF/EE flocs (open fabric), and in turn, higher liquid limit. In addition, polymer molecules provided additional adsorption sites for water molecules, also contributing to the higher liquid limit. As the number of monomer unit increased (with higher molecular mass and higher concentration), the number of polymer adsorption sites also increased.

This study indicates that kaolin clay fabric can be successfully modified with the use of polyacrylamide. Once kaolin fabric is manipulated, the structure is retained due to the irreversible adsorption of polyacrylamide molecule to the mineral surface. The influence of polyacrylamide on kaolin fabric, particle association type, and number of associations that develop depends on the molecular mass, concentration, and ion type of the polymer as function of the solids content of the system. This study of polymer–clay combination offers a new outlook for purpose of creating engineered soil systems.

References

ASTM, 2003. D422-63: Standard Test Method for Particle-Size Analysis of Soils. American Society for Testing and Materials (ASTM).

Backfolk, K., Rosenholm, J.B., Husband, J., Eklund, D., 2006. The influence of surface chemical properties of kaolin surfaces on the adsorption of poly(vinyl alcohol). Colloids and Surfaces. A, Physicochemical and Engineering Aspects 275 (1–3), 133–141.

Bhatty, J.I., Dollimore, D., Zahedi, A.H., 1978. The aggregation of kaolinite suspensions in gum tragacanth solutions. Transactions and journal of the British Ceramic Society 77 (4), 126–131.

Borden, D., Giese, R.F., 2001. Baseline studies of the clay minerals society source clays: cation exchange capacity measurements by the ammonia-electrode method. Clays and Clay Minerals 49 (5), 444–445.

Brandrup, J., Immergut, E.H., 1989. Polymer Handbook, 3rd ed. Wiley, New York.

BSI, 1990. BS1377-90 Section 4: Determination of Liquid Limit. British Standards Institution (BSI).

Carasso, M.L., Rowlands, W.N., O'Brien, R.W., 1997. The effect of neutral polymer and nonionic surfactant adsorption on the electroacoust signals of colloidal silica. Journal of Colloid and Interface Science 193 (2), 200–214.

Chaplain, V., Janex, M.L., Lafuma, F., Graillat, C., Audebert, R., 1995. Coupling between polymer adsorption and colloidal particle aggregation. Colloid & Polymer Science 273 (10), 984–993.

Dollimore, D., Horridge, T.A., 1973. The dependence of the flocculation behavior of china clay–polyacrylamide suspensions on the suspension pH. Journal of Colloid and Interface Science 42 (3), 581–588.

Ebnesajjad, S., 2006. Surface Treatment of Materials for Adhesion Bonding. William Andrew Pub., New York.

Fleer, G.J., Koopal, L.K., Lyklema, J., 1972. Polymer adsorption and its effect on the stability of hydrophobic colloids. Colloid & Polymer Science 250 (7), 689–702.

Font, R., Garcia, P., Rodriguez, M., 1999. Sedimentation test of metal hydroxides: hydrodynamics and influence of pH. Colloids and Surfaces. A, Physicochemical and Engineering Aspects 157 (1–3), 73–84.

Godard, K., Richardson, J.F., 1969. Correlation of data for minimum fluidising velocity and bed expansion in particularly fluidised systems. Chemical Engineering Science 24 (2), 363–367.

Gregory, J., 1988. Polymer adsorption and flocculation in sheared suspensions. Colloids and Surfaces 31, 231–253.

Huang, S.-Y., Lipp, D.W., Farinato, R.S., 2001. Acrylamide Polymers, Kirk-Othmer Encyclopedia of Chemical Technology.

Hunter, R.J., 1993. Introduction to Modern Colloid Science, 1st ed. Oxford University Press, Oxford.

Hunter, R.J., 2001. Foundations of Colloid Science, 2nd ed. Oxford University Press, Oxford.

Irani, R.R., Callis, C.F., 1963. Particle Size: Measurement, Interpretation, and Application. Wiley, New York.

Israelachvili, J.N., 1991. Intermolecular and Surface Forces, 2nd ed. Academic Press, London.

Kaya, A., Oren, A.H., Yukselen, Y., 2006. Settling of kaolinite in different aqueous environment. Marine Georesources and Geotechnology 24 (3), 203–218.

Kim, S., 2008. Polyacrylamide-Treated Kaolin Clay: A Fabric Study, Master's Thesis, Penn State University, University Park, U.S.A., 90 p.

Kretzschmar, R., Holthoff, H., Sticher, H., 1998. Influence of pH and humic acid on coagulation kinetics of kaolinite: a dynamic light scattering study. Journal of Colloid and Interface Science 202 (1), 95–103.

Lagaly, G., 2006. Colloid clay science. In: Bergaya, F., Theng, B.K.G., Lagaly, G. (Eds.), Handbook of clay science. InElsevier, Boston, pp. 141–245.

Laird, D.A.D., 1997. Bonding between polyacrylamide and clay mineral surfaces. Soil science 162 (11), 826–832.

Ma, C., Eggleton, R.A., 1999. Cation exchange capacity of kaolinite. Clays and Clay Minerals 47 (2), 174–180.

Mitchell, J.K., 1956. The fabric of natural clays and its relation to engineering properties. 35th Annual Meeting, Washington, D.C. In: Highway Research Board Proceedings, vol. 35, pp. 693–713.

Mitchell, J.K., 1993. Fundamentals of Soil Behavior, 2nd ed. John Wiley & Sons, New York.

Mitchell, J.K., Soga, K., 2005. Fundamentals of Soil Behavior, 3rd ed. John Wiley & Sons.

Mpofu, P., Addai-Mensah, J., Ralston, J., 2003. Investigation of the effect of polymer structure type on flocculation, rheology and dewatering behaviour of kaolinite dispersions. International Journal of Mineral Processing 71 (1–4), 247–268.

Murray, H.H., 1991. Overview — clay mineral applications. Applied Clay Science 5, 379–395.

Palomino, A.M., Santamarina, J.C., 2005. Fabric map for kaolinite: effects of pH and ionic concentration on behavior. Clays and Clay Minerals 53 (3), 209–222.

Pefferkorn, E., Nabzar, L., Carroy, A., 1985. Adsorption of polyacrylamide to Na kaolinite: correlation between clay structure and surface properties. Journal of Colloid and Interface Science 106 (1), 94–103.

Penner, D., Lagaly, G., 2000. Influence of organic and inorganic salts on the coagulation of montmorillonite dispersions. Clays and Clay Minerals 48 (2), 246–255.

Pierre, A.C., Ma, K., Barker, C., 1995. Structure of kaolinite flocs formed in an aqueous medium. Journal of Materials Science 30 (8), 2176–2181.

Rand, B., Melton, I.E., 1977. Particle interactions in aqueous kaolinite suspensions i. effect of pH and electrolyte upon the mode of particle interaction in homoionic sodium kaolinite suspensions. Journal of Colloid and Interface Science 60 (2), 308–320.

Ravve, A., 2000. Principles of Polymer Chemistry, 2nd ed. Kluwer Academic/Plenum Publishers, New York.

Richardson, J.F., Zaki, W.N., 1954. Sedimentation and fluidisation: Part 1. Transactions of the Institution of Chemical Engineers 32 (1), 35–53.

Santamarina, J.C., Klein, K.A., Wang, Y.H., Prencke, E., 2002. Specific surface: determination and relevance. Canadian Geotechnical Journal 39 (1), 233–241.

Theng, B.K.G., 1979. Formation and Properties of Clay–Polymer Complexes. New York, Amsterdam.

van Olphen, H., 1977. An Introduction to Clay Colloid Chemistry: For Clay Technologists, Geologists, and Soil Scientists, 2nd ed. Wiley, New York.

Williams, B.G., Drover, D.P., 1967. Factors in gel formation in soil suspensions. Soil Science 104 (5), 326–331.

Wroth, C.P., Wood, D.M., 1978. The correlation of index properties with some basic engineering properties of soils. Canadian Geotechnical Journal 15 (2), 137–145.